

OPEN

Neurology®

The most widely read and highly cited peer-reviewed neurology journal  
The Official Journal of the American Academy of Neurology



Neurology Publish Ahead of Print  
DOI: 10.1212/WNL.0000000000010645

## Thalamus and focal to bilateral seizures: A multi-scale cognitive imaging study

Lorenzo Caciagli, MD, PhD,<sup>1,2,3</sup> Luke A. Allen, PhD,<sup>1,2</sup> Xiaosong He, PhD,<sup>3</sup> Karin Trimmel, MD, PhD,<sup>1,2,4</sup> Sjoerd B. Vos, PhD,<sup>1,2,5,6</sup> Maria Centeno, MD, PhD,<sup>1,2</sup> Marian Galovic, MD,<sup>1,2,7</sup> Meneka K. Sidhu MB, ChB PhD,<sup>1,2</sup> Pamela J. Thompson, PhD,<sup>1,2</sup> Danielle S. Bassett, PhD,<sup>3,8,9,10,11,12</sup> Gavin P. Winston BM BCh, PhD, FRCP,<sup>1,2,13</sup> John S. Duncan, DM, FRCP, FMedSci,<sup>1,2</sup> Matthias J. Koepp MD, PhD, FRCP,<sup>1,2</sup> Michael R. Sperling, MD<sup>14</sup>

The Article Processing Charge was funded by the Wellcome Trust.

This is an open access article distributed under the terms of the Creative Commons Attribution License 4.0 (CC BY), which permits unrestricted use, distribution, and reproduction in any medium, provided the original work is properly cited.

*Neurology*® Published Ahead of Print articles have been peer reviewed and accepted for publication. This manuscript will be published in its final form after copyediting, page composition, and review of proofs. Errors that could affect the content may be corrected during these processes.

<sup>1</sup>*Department of Clinical and Experimental Epilepsy, UCL Queen Square Institute of Neurology, Queen Square, London WC1N 3BG, United Kingdom*

<sup>2</sup>*MRI Unit, Epilepsy Society, Chalfont St Peter, Buckinghamshire, SL9 0RJ, United Kingdom*

<sup>3</sup>*Department of Bioengineering, University of Pennsylvania, 240 South 33<sup>rd</sup> Street, Philadelphia, Pennsylvania, USA*

<sup>4</sup>*Department of Neurology, Medical University of Vienna, Vienna, Austria*

<sup>5</sup>*Centre for Medical Image Computing, University College London, London, United Kingdom*

<sup>6</sup>*Neuroradiological Academic Unit, UCL Queen Square Institute of Neurology, Queen Square, London WC1N 3BG, United Kingdom*

<sup>7</sup>*Department of Neurology, University Hospital Zurich, Switzerland*

<sup>8</sup>*Department of Physics and Astronomy, University of Pennsylvania, Philadelphia, Pennsylvania, USA*

<sup>9</sup>*Department of Electrical and Systems Engineering, University of Pennsylvania, Philadelphia, Pennsylvania, U.S.A.*

<sup>10</sup>*Department of Neurology, University of Pennsylvania, Philadelphia, Pennsylvania, USA*

<sup>11</sup>*Department of Psychiatry, University of Pennsylvania, Philadelphia, Pennsylvania, USA*

<sup>12</sup>*Santa Fe Institute, Santa Fe, New Mexico, USA*

<sup>13</sup>*Department of Medicine, Division of Neurology, Queen's University, Kingston, Ontario, Canada*

<sup>14</sup>*Department of Neurology, Thomas Jefferson University, 901 Walnut Street, Philadelphia, Pennsylvania, USA*

**Correspondence to:** Dr Lorenzo Caciagli, [lorenzo.caciagli.11@ucl.ac.uk](mailto:lorenzo.caciagli.11@ucl.ac.uk)

**Submission Type:** Article

**Search Terms:** (1) Temporal lobe epilepsy; (2) secondary generalization; (3) thalamus; (4) fMRI; (5) language.

**79** characters in Title; **245** words in Abstract, **4499** words in Manuscript Body, **50** References; **5** Color Figures, **2** Tables.

**Supplemental Data available on Dryad (<https://doi.org;10.5061/dryad.2bvq83bm8>):** 2 e-Appendices, 2 e-Figures, 2 e-Tables, 16 e-References

**Statistical analysis** conducted by Dr. Lorenzo Caciagli, MD, PhD, UCL Queen Square Institute of Neurology, London, UK; MRI Unit, Epilepsy Society, Chalfont St Peter, Buckinghamshire; and Department of Bioengineering, University of Pennsylvania, Philadelphia, USA.

## STUDY FUNDING

The study was funded through the Wellcome Trust (Project Grants No 079474 and 083148). The Epilepsy Society supported the Epilepsy Society MRI scanner. This research was also supported by the National Institute for Health Research University College London Hospitals Biomedical Research Centre. LC was funded by a PhD scholarship from Brain Research UK (Award reference 14181) and acknowledges previous support by an Ermenegildo Zegna Founder's Scholarship. KT was supported by fellowships of the European Academy of Neurology and the Austrian Society of Neurology (OEGN). MKS is supported by the National Institute for Health Research University College London Hospitals Biomedical Research Centre. D.S.B. acknowledges support from the John D. and Catherine T. MacArthur Foundation, the Alfred P. Sloan Foundation, the ISI Foundation, and NINDS R01-NS099348-01. GPW was supported by an MRC Clinician Scientist Fellowship (MR/M00841X/1). The funders had no role in study design, data collection and analysis, decision to publish, or preparation of the manuscript.

## DISCLOSURE

L. Caciagli, L. Allen, X. He, K. Trimmel, S. Vos, M. Centeno, M. Galovic, M. Sidhu, P. Thompson, and D. Basset report no disclosures relevant to the manuscript.

G. Winston reports grant funding from the Medical Research Council during the conduct of the study.

J. Duncan and M. Koepp report no disclosures relevant to the manuscript.

M. Sperling reports grants from Medtronic, UCB Pharma, Takeda, Neurelis, SK Life Science, Engage Therapeutics and Eisai outside the submitted work.

## ABSTRACT

### *Objective*

To investigate the functional correlates of recurrent secondarily generalized seizures in temporal lobe epilepsy (TLE), using task-based fMRI as a framework to test for epilepsy-specific network rearrangements. As the thalamus modulates propagation of temporal-lobe

onset seizures and promotes cortical synchronization during cognition, we hypothesized that occurrence of secondarily generalized, i.e. focal to bilateral tonic-clonic seizures (FBTCS), would relate to thalamic dysfunction, altered connectivity and whole-brain network centrality.

### ***Methods***

FBTCS occur in a third of patients with TLE and are a major determinant of disease severity. In this cross-sectional study, we analyzed 113 patients with drug-resistant TLE (55 left/58 right), who performed a verbal fluency fMRI task that elicited robust thalamic activation. Thirty-three patients (29%) had experienced at least one FBTCS in the year preceding the investigation. We compared patients with TLE-FBTCS to those without FBTCS via a multi-scale approach, entailing analysis of SPM12-derived measures of activation, task-modulated thalamic functional connectivity (psychophysiological interaction), and graph-theoretical metrics of centrality.

### ***Results***

Individuals with TLE-FBTCS had less task-related activation of bilateral thalamus, with left-sided emphasis, and left hippocampus than those without FBTCS. In TLE-FBTCS, we also found greater task-related thalamotemporal and thalamo-motor connectivity, and higher thalamic degree and betweenness centrality. Receiver operating characteristic curves, based on a combined thalamic functional marker, accurately discriminated individuals with and without FBTCS.

### ***Conclusions***

In TLE-FBTCS, impaired task-related thalamic recruitment coexists with enhanced thalamotemporal connectivity and whole-brain thalamic network embedding. Altered thalamic functional profiles are proposed as imaging biomarkers of active secondary generalization.

## INTRODUCTION

Temporal lobe epilepsy (TLE) is the most common focal epilepsy syndrome in adults. Focal to bilateral tonic-clonic seizures (FBTCS), formerly termed secondarily-generalized seizures, affect at least a third of people with TLE,<sup>1</sup> are a major risk factor for seizure-related injuries and sudden unexpected death in epilepsy (SUDEP),<sup>2,3</sup> and a predictor of unfavorable post-surgical outcome.<sup>4</sup> Why some people experience these seizures while others do not remains poorly understood. Presumably, specific functional and structural rearrangements may underlie the propensity for large-scale propagation of epileptic activity underlying this severe seizure type. Enhancing our understanding of the mechanisms leading to FBTCS may provide insight into much-needed novel therapeutic targets.

In TLE, thalamic atrophy represents the most common extra-temporal abnormality<sup>5,6</sup> and relates to derangements of cortico-subcortical connectivity,<sup>6,7</sup> with unfavorable implications for post-surgical outcome.<sup>8,9</sup> Converging evidence indicates that subcortical nuclei, particularly the thalamus, may be involved in the propagation of temporal lobe seizures.<sup>10,11</sup> Resting-state functional MRI (fMRI) analyses detected more widespread thalamocortical abnormalities in patients with TLE and FBTCS, compared to those with focal seizures that do not generalize (TLE-FS).<sup>12</sup> Recent work also identified impairment of thalamotemporal structural connections in TLE-FBTCS.<sup>13</sup>

The thalamus contributes to motor planning, language and memory by promoting cortical synchronization and facilitating cortico-cortical interplay.<sup>14,15</sup> Cognitive tasks perturb brain network dynamics and evoke complex changes in interregional interactions,<sup>16</sup> offering a powerful tool to identify disease-specific network traits<sup>17</sup> that resting-state analyses may not adequately capture.<sup>18</sup> *In vivo*, cognition is probed via task-based fMRI. Verbal fluency tasks assess expressive language, and allow ascertaining language lateralization in focal epilepsy.<sup>19</sup> Typical activation patterns encompass fronto-temporo-parietal cortices, mesiotemporal structures and, notably, bilateral thalamus, with left-sided emphasis.<sup>20,21</sup>

Thus, by challenging robustness of a functional network largely overlapping with the putative epileptogenic network of TLE, fluency-related task-fMRI provides a powerful framework for assessing intergroup differences in underlying brain network organization. If the occurrence of FBTCS in TLE is related to abnormal thalamocortical interactions, then, one may expect to detect abnormal thalamic activation and connectivity with cognitive demand.

Here, we pursued a comprehensive characterization of the functional underpinnings of recurrent secondary generalization in TLE. As distinct from previous investigations, we envisioned the use of task-based fMRI to capture specific, FBTCS-associated rearrangements within networks recruited during linguistic processing. We hypothesized that, compared to TLE-FS, TLE with recent FBTCS would exhibit impaired thalamic activation, altered connectivity between thalamus and key symptomatogenic areas, including mesiotemporal and motor regions, and higher overall thalamic relevance for mediating signals within large-scale networks. To test these hypotheses, we employed a verbal fluency fMRI paradigm and a multi-scale approach entailing comparison of TLE-FS and FBTCS across (1) task-related activation, (2) task-modulated changes of thalamic functional connectivity, via a psychophysiological interaction analysis, and (3) graph-theoretical measures of thalamic centrality. Innovatively, we also linked domains of activation, connectivity and centrality via a composite thalamic functional marker, and investigated its potential to discriminate TLE-FS and FBTCS at the individual level.

## METHODS

### *Participants (Table 1)*

For this cross-sectional investigation, we consecutively recruited 113 patients with drug-resistant TLE [55 left (30 females); 58 right (43 females)], who underwent presurgical evaluation at the National Hospital for Neurology and Neurosurgery (NHNN), London, UK, between 2008 and 2014. All subjects underwent prolonged interictal and ictal scalp video-EEG, confirming and lateralizing the epileptic focus to one temporal lobe, and presurgical 3T-MRI, with qualitative assessment and quantification of hippocampal volumetry and T2 relaxometry.<sup>22</sup> Ipsilateral MRI findings included hippocampal sclerosis [n=32/29, left TLE (LTLE)/right TLE (RTLE)], dysembryoplastic neuroepithelial tumor (DNET; n=5/8, LTLE/RTLE), cavernoma (n=4/7, LTLE/RTLE), and normal-appearing MRI (n=14/14, LTLE/RTLE). Contralateral mesiotemporal structures were normal in all cases. History of affective illness, referring to depressive and anxiety disorders, was recorded as detailed previously.<sup>23</sup> Additional clinical/demographic details are available in *Appendix e-1*.

Thirty-three patients (29.2%; 20/13, LTLE/RTLE) had experienced at least one FBTCS during the year preceding the investigation (median frequency/month: 0.46, interquartile range: 0.83), and were therefore considered as having a *current* tendency for FBTCS

(henceforth referred to as “TLE-FBTCS”). This one-year cut-off for subgroup allocation was envisioned to probe the neural correlates of recent, active secondary generalization, and relies on multiple lines of evidence specifically linking generalized seizures in the last year to SUDEP risk,<sup>2,3</sup> or recommending assessment of seizure-freedom in the last year for clinical outcome classification.<sup>24</sup> However, we also conducted *post-hoc* analyses on three groups, after subdividing the main TLE-FS group into: (1) TLE without lifetime history of FBTCS (*never-FBTCS*, n=38; 14/24, left/right), and (2) TLE with history of remote FBTCS, but none for >1 year before scanning (*remote-FBTCS*, n=42; 21/21, left/right).

#### Standard Protocol Approvals, Registrations and Patient Consents

This study was approved by the NHNN and UCL Institute of Neurology Joint Research Ethics Committee. Written informed consent was obtained from all subjects.

#### Data acquisition and fMRI task specifics

All participants underwent neuropsychological tests measuring intellectual level (IQ), letter and category fluency, and visual confrontation naming. We also evaluated group comparability for processing speed and executive function (Table 1, *Appendix e-1*). The Beck Depression Inventory-Fast Screen and Beck Anxiety Inventory measured mood and anxiety. Handedness was determined using the Edinburgh Handedness Inventory. T1-weighted and fMRI data were acquired on a 3T GE Signa-HDx MRI scanner using previously-described protocols (*Appendix e-1*).<sup>25</sup> Automated hippocampal and thalamic volumetric measures were available for all subjects. All participants performed a verbal fluency paradigm lasting 5 minutes, consisting of 30s task blocks requiring subjects to covertly generate words beginning with a visually-presented letter (A/D/E/S/W; one letter per block, 5 blocks in total), alternating with 30s blocks of cross-hair fixation.<sup>26</sup>

#### Analysis of clinical and neuropsychological data

For all main analyses on two TLE groups (TLE-FBTCS versus TLE-FS), we used Fisher’s exact test, two-sample *t*-test and Mann-Whitney *U*-test for categorical, continuous parametric and non-parametric variables, respectively. Correction for multiple comparisons was attained with the False Discovery Rate (FDR) procedure. Additional analyses comparing FS and

FBTCS patients were separately carried out for LTLE and RTLE subgroups. Details regarding *post-hoc* analyses on three groups (TLE-FBTCS, *remote*-FBTCS and *never*-FBTCS) are provided at the end of the *Methods* section.

#### Imaging data analysis: fMRI activation

We analyzed fMRI data with Statistical Parametric Mapping (SPM) 12 using previously-detailed pipelines (*Appendix e-1*).<sup>25</sup> Four subjects were excluded owing to corrupted field of view (n=1) or excessive motion (> |3| mm and/or |3| degrees overall; n=3). For each participant, we computed voxel-wise parameter estimates and contrast images for task-related activation, including motion parameters as confounds. At the second level, one-sample *t*-tests assessed fluency-related effects across all subjects. Two-sample *t*-tests assessed differences between TLE-FBTCS and TLE-FS, with lateralization of the epileptic focus as covariate. Subgroup analyses separately compared LTLE-FS to LTLE-FBTCS, and RTLE-FS to RTLE-FBTCS. Age and sex were used as covariates in all group comparisons. Sensitivity analyses entailed repeat group comparisons with letter fluency scores as nuisance regressors. Task effects were thresholded at  $p < 0.05$ , corrected for multiple comparisons [family-wise error rate, (FWE)] across the whole brain. In view of our *a priori* hypotheses, group differences were considered significant at  $p < 0.05$ , FWE-corrected within a region of interest (ROI) consisting of a 12mm diameter sphere (small volume correction, “FWE-svc”) centered at the location of the maxima for thalamus, hippocampus and motor areas [precentral gyrus, supplementary motor area (SMA)].<sup>27</sup> For completeness, we report whole-brain effects at an exploratory threshold of  $p < 0.005$  uncorrected with a 20-voxel minimum cluster-size threshold ( $p < 0.005$ ,  $k=20$ ).<sup>28,29</sup> To convey higher spatial details for our thalamic findings, locations of activation and group difference maxima were related to thalamic sub-nuclei using the digital version of the Morel stereotactic atlas of the human thalamus.<sup>30</sup> Hemispheric dominance for frontal and thalamic activation was determined via laterality indices of statistical parametric maps (*Appendix e-1*).

#### Multiple regression models on thalamic activation

We assessed determinants of task-related thalamic activation via multiple regression models, conducted with R-3.4.4. We extracted parameter estimates of thalamic activation from an independent ROI, represented by the ventral anterior nucleus (*parvocellular part*) of the

Morel atlas,<sup>30</sup> and used the following independent variables: occurrence of FBTCS in the last year, focal seizure frequency (log), sex, handedness, lateralization of the epileptic focus, number of anti-epileptic drugs, and affective history. For dimensionality reduction, measures of verbal fluency (letter/category fluency) and disease load (age at onset, disease duration) were entered into principal component analyses (PCAs; *Appendix e-1*). Both first principal components (“fluency” and “chronicity”) were then implemented as additional regressors.

#### Task-related functional connectivity: psychophysiological interactions

We probed thalamic connectivity with a psychophysiological interaction (PPI) analysis,<sup>31</sup> testing whether connection strength between a pre-specified seed region and other brain areas was modulated by task execution. Individual fMRI time-series were obtained from the preprocessed images using a 12-mm diameter sphere centered on individual, subject-specific left and right anterior thalamic peak activation voxels (*Appendix e-1*).<sup>32</sup> The PPI general linear model included three regressors: (1) main effect of the seed region (i.e., the functional time-series), (2) task regressor (i.e., “psychological factor”, represented by the vector of the word-generation block onset) and (3) interaction of the former two, representing a task-modulated change in connectivity, or PPI.<sup>31</sup> Motion parameters were included as nuisance regressors. One-sample *t*-tests identified areas exhibiting task-related connectivity changes with the thalamic seeds. Two-sample *t*-tests compared TLE-FBTCS and TLE-FS groups, as well as left and right TLE subgroups. Main PPI effects were thresholded at  $p < 0.05$ , FWE-corrected across the whole brain. In view of our *a priori* hypotheses, group differences were considered significant at  $p < 0.05$ , FWE-corrected within a 12mm-diameter sphere (FWE-svc) centered at the maxima in the hippocampus and motor areas.<sup>27</sup> For completeness, whole-brain effects are reported at an exploratory statistical threshold of  $p < 0.005$ ,  $k = 20$ .<sup>28,29</sup>

#### Graph-theoretical analysis

Further image processing included regression of nuisance variables, band-pass filtering (0.01 to 0.1 Hz) and removal of the superimposed blocked task structure via condition-specific regressors, in line with benchmark evidence (*Appendix e-1*). Regional parcellation was attained via the *Brainnetome* atlas (246 ROI).<sup>33</sup> After extracting ROI-averaged time series, we computed absolute Pearson correlation coefficients for every possible ROI pair, obtaining a 246x246 connectivity matrix for each participant. Weighted matrices were thresholded and

binarized at network densities between 5% and 40% in increments of 1%, yielding 36 binary undirected graphs per subject. Bilateral thalamic parcels (regions 231/232, corresponding to a left/right anterior thalamic division) were identified as nodes for network statistics. We investigated measures of centrality (*hubness*), in light of their relevance for clinical outcome prediction in TLE.<sup>9</sup> For each node at each network density, we computed (1) *degree centrality*, describing the number of connections of a given node, and (2) *betweenness centrality*, describing the frequency with which a given node is located on the shortest path between other node pairs. Differences in thalamic centrality between TLE-FBTCS and TLE-FS, and for left and right TLE subgroups, were assessed via (1) comparisons of mean metric values, obtained after averaging across densities,<sup>34</sup> and followed up with (2) subsequent contrasts for each network density value for each metric. We used non-parametric permutation tests entailing 10000 permutations for each comparison, which generated permuted *t*-statistic distributions with associated *p*-values,<sup>9</sup> followed by FDR-adjustment for multiple testing ( $p_{\text{FDR}} < 0.05$ ; *Appendix e-1*).

#### ROC curves with thalamic functional markers

ROC curves assessed the accuracy with which age- and sex-adjusted thalamic functional metrics could discriminate between TLE-FBTCS and TLE-FS. Initial models implemented markers of activation, extracted from the ventral anterior thalamic parcel of the Morel atlas. To characterize the additional contribution of connectivity and graph metrics, ROC curve analyses were repeated using a composite functional construct, obtained after PCA on measures of activation, task-based connectivity and centrality (*Appendix e-1*). Logistic regressions quantified the additive discriminative potential of activation and connectivity metrics. Models were compared via likelihood-ratio tests.

#### Post-hoc analyses on three TLE groups

*Post-hoc* analyses examined TLE with (current) FBTCS, TLE *remote*-FBTCS and TLE *never*-FBTCS regarding parameter estimates of thalamic and hippocampal activation, thalamotemporal and thalamo-motor task-related connectivity, degree and betweenness centrality. Across all analyses, we specifically tested the hypothesis that altered thalamic network embedding would relate to a current propensity for secondary generalization and, consequently, that there would be no significant differences between *remote*-FBTCS and

*never*-FBTCS individuals. Subgroups were compared via multivariate and univariate ANOVA, along with non-parametric permutation ANOVA for graph-theoretical metrics. Extraction of activation and connectivity metrics and statistical procedures are detailed in *Appendix e-1*.

#### Data Availability

Data supporting our findings are available from the corresponding author upon reasonable request.

## RESULTS

#### Demographic and clinical characteristics

There were no differences between TLE-FS and TLE-FBTCS for demographic and clinical variables, including temporal pathology subtype, number of AEDs and usage of topiramate or zonisamide, which both affect verbal fluency activations<sup>28</sup> (all  $p > 0.05$ ; Table 1). Subgroup analyses, comparing LTLE-FBTCS against LTLE-FS, and RTLE-FBTCS against RTLE-FS, identified no significant differences. Propensity for FBTCS was similar in LTLE and RTLE subgroups ( $\chi^2 = 2.66$ ,  $p = 0.10$ ). A history of comorbid affective disorders was documented for 36.3% and 45.5% of TLE-FS and TLE-FBTCS patients, respectively, with no group differences. Scores for anxiety and depression symptoms and usage of anti-depressant/anxiolytic medication did not differ between groups (Table 1; *Appendix e-2*).

#### Cognitive measures and volumetric findings

There were no differences between TLE-FBTCS and TLE-FS for all cognitive measures, thalamic and hippocampal volumes (all  $p > 0.05$ ; Table 1). Subgroup analyses detected a difference between LTLE-FBTCS and LTLE-FS regarding letter fluency scores, with LTLE-FBTCS outperforming LTLE-FS ( $p_{FDR} = 0.01$ ). Consequently, sensitivity analyses addressed confounding effects of fluency performance on imaging metrics. Additional analyses indicated that differences in letter fluency between LTLE-FS and LTLE-FBTCS were largely mediated by hippocampal volume, processing speed and medication, all of which had no influence on thalamic activation, connectivity and graph-theoretical metrics (linear regression

models, all variables  $p > 0.23$ ; *Appendix e-2*). There were no other significant differences for cognitive and volumetric measures between LTLE and RTLE subgroups.

### Verbal fluency fMRI: activation-based analysis

The task elicited the expected<sup>28</sup> activation of language-relevant fronto-temporo-parietal cortices, hippocampus, putamen and pallidum with left-sided emphasis, as well as right cerebellum (Figure 1A). Thalamic activation encompassed bilateral anterior divisions and left-sided posterior nuclei, with local maxima in the ventral anterior parcel of the Morel atlas. Patients with TLE-FBTCS had less task-related activation of bilateral anterior and posterior thalamus and left anterior hippocampus than TLE-FS patients ( $p < 0.05$ , FWE-svc; Figure 1B; Table 2). Peak thalamic activation differences fell within ventral anterior nuclei; additional peaks were detected in the centrolateral/lateral posterior group. Exploratory whole-brain analyses detected lower activation in TLE-FBTCS in bilateral posterior parahippocampal gyrus and subcortical structures (Figure 1B, second row) including putamen, pallidum, cerebellum, and subthalamus. Sensitivity analyses controlling for fluency performance did not affect anterior thalamic findings, but reduced significance of hippocampal and right posterior thalamic differences (Table 2). There was no increased activation in TLE-FBTCS compared to TLE-FS.

*Post-hoc* analyses contrasted TLE subgroups with a sample of 53 healthy controls, balanced for demographic variables (*Appendix e-1*). Thalamic activation was comparable to controls in TLE-FS, and significantly lower in TLE-FBTCS (all  $p_{FDR} < 0.0003$ ), while hippocampal activation appeared reduced in both groups, with subtle effects in TLE-FS ( $p = 0.015$ , uncorrected;  $p_{FDR} = 0.075$ ), and marked changes in TLE-FBTCS ( $p_{FDR} < 0.0001$ ; *Figure e-1*, *Appendix e-2*).

Subgroup analyses detected reduced activation of bilateral anterior thalamus, left posterior thalamus and bilateral hippocampus in LTLE-FBTCS compared to LTLE-FS ( $p < 0.05$ , FWE-svc; Figure 1C; Table e-1). The sub-regional distribution of thalamic differences was similar to the main analysis, with ventral anterior maxima, and exploratory whole-brain comparisons in LTLE-FBTCS showed hypoactivation of the same widespread subcortical areas described for the main analysis. Repeat models controlling for fluency performance did not affect subgroup findings. In RTLE, thalamic differences between FBTCS and FS were not significant (Figure 1D).

Collectively, our findings indicate thalamic and hippocampal hypoactivation on verbal fluency fMRI in TLE-FBTCS.

#### Multiple regression analysis on activation metrics

Multiple regression based on the full predictor set was significant ( $F_{(9,93)}=3.17$ ,  $p=0.002$ ; multiple  $R^2=0.23$ , adjusted  $R^2=0.16$ ). Occurrence of FBTCS in the last year was the most significant determinant of thalamic activation, and the association was negative [ $\beta=-0.17$ , 95% confidence interval (CI)= (-0.28, -0.05),  $t=-2.90$ ,  $p=0.005$ ]. Handedness, sex, and side of epilepsy also had significant effects [ $\beta$ s=-0.19/-0.13/-0.11, 95% CI= (-0.35, -0.04)/(-0.24, -0.01)/(-0.22, -0.005),  $t=-2.53/-2.24/-2.06$ ,  $p=0.013/0.027/0.041$ , respectively]. Interaction terms (FBTCS\*handedness, FBTCS\*lateralization, FBTCS\*sex) were non-significant (all  $p>0.05$ ).

#### Psychophysiological interaction analysis

PPI analysis showed task-modulated connectivity changes between the left thalamic ROI and fronto-temporo-parietal cortices, contralateral thalamus, basal ganglia and mesiotemporal lobes (Figure 2A). Overlapping effects were identified for PPI analysis from the right thalamus (Figure 3A). In both cases, task-modulated changes in connectivity were negative, implying reduced thalamic functional connectivity (i.e., thalamocortical decoupling) as a function of task performance, in accord with previous evidence.<sup>35</sup>

Compared to TLE-FS, TLE-FBTCS exhibited less attenuated task-dependent connectivity (i.e., failure to reduce coupling) between left thalamus and both (a) left hippocampus, and (b) motor areas, including bilateral precentral gyrus and right SMA ( $p<0.05$ , FWE-svc; Figure 2B; Table 2). Additional whole-brain effects were detected in left posterior insula/operculum, right superior frontal and anterior cingulate cortices. Stronger task-dependent left thalamic connectivity to left hippocampus, contralateral thalamus and motor areas was observed in LTLE-FBTCS compared to LTLE-FS, whereas significant differences only encompassed thalamo-motor connections in RTLE-FBTCS versus FS ( $p<0.05$ , FWE-svc; Figure 2C, 2D; Table e-1). Controlling for verbal fluency performance increased statistical significance of all group comparisons (Tables 2, e-1).

Similarly, PPI analyses from the *right* thalamus highlighted less attenuated connectivity to left hippocampus and amygdala in TLE-FBTCS compared to TLE-FS ( $p < 0.05$ , FWE-svc; Figure 3B; Table 2). Subgroup analyses showed higher connectivity to the left hippocampus in LTLE-FBTCS compared to LTLE-FS, and additional whole-brain effects were identified for the right putamen (Figure 3C; Table e-1). In RTLE-FBTCS, stronger connectivity to left amygdala and right hippocampus was evident at uncorrected thresholds. Sensitivity analyses controlling for linguistic performance amplified the above-described effects.

Collectively, our results point to enhanced task-related thalamotemporal and thalamo-motor interactions in TLE-FBTCS.

### Graph-theoretical findings

TLE-FBTCS showed significantly higher mean betweenness centrality of bilateral thalamus and higher mean right degree compared to TLE-FS (uncorrected  $p = 0.037/0.033/0.032$ , respectively; all  $p_{FDR} = 0.049$ , adjusted across four measures). Differences for left degree were not significant ( $p_{FDR} = 0.10$ ). Regarding the former significant measures, higher centrality in TLE-FBTCS was apparent across most network densities (Figure 4). Subgroup analyses showed higher left thalamic betweenness centrality in LTLE-FBTCS compared to FS at the uncorrected level, both for mean values ( $p = 0.029$  uncorrected,  $p_{FDR} = 0.12$ ) and across network densities, and significantly higher right thalamic degree in RTLE-FBTCS versus RTLE-FS ( $p = 0.008$  uncorrected,  $p_{FDR} = 0.030$ ). Inspection of plots for the remaining non-significant comparisons showed overall trends for higher centrality in FBTCS subgroups.

### Individual discrimination via thalamic functional measures

ROC curve analyses based on anterior thalamic activation discriminated between TLE-FBTCS and TLE-FS individuals [AUC=0.67, (95% CI=0.56-0.77),  $p = 0.007$ ]. Subgroup analyses detected higher discrimination of LTLE subgroups [AUC=0.69 (0.55-0.83),  $p = 0.026$ ], while findings in RTLE approached significance [AUC=0.67 (0.52-0.83),  $p = 0.06$ ]. Usage of a composite functional marker, incorporating activation, task-related connectivity and graph-theory metrics, achieved substantially higher discrimination than activation measures alone [ROC curve on combined metric, AUC=0.75 (0.64-0.85),  $p < 0.0001$ ]. Effects were more prominent for LTLE [AUC=0.83 (0.70-0.95),  $p = 0.0001$ ], and also significant in RTLE [AUC=0.73 (0.58-0.89),  $p = 0.011$ ]. Comparison of logistic regressions via likelihood-

ratio tests (*Appendix e-1*) identified marked additive contributions of task-related connectivity to subgroup discrimination ( $p=0.006$ ), whilst addition of graph-theoretical metrics to the former two only yielded marginal improvements in model fit ( $p>0.10$ ).

### Post-hoc analyses on three TLE groups

MANOVA on measures of activation, left and right PPI identified no significant differences between TLE *never*-FBTCS and *remote*-FBTCS ( $p=0.25/0.60/0.63$ , respectively;  $p>0.23$  for all univariate analyses). MANOVA on three groups, on the other hand, confirmed significant effects for thalamic activity, left and right PPI ( $p=0.016/0.021/0.013$ , respectively; all  $p_{FDR}=0.021$ ), with corrected univariate *post-hoc* analyses (Tukey's test) detecting differences for comparison of TLE-FBTCS versus either TLE *never*-FBTCS, or TLE *remote*-FBTCS, or both (Figure 5; Table e-2).

Analysis of thalamic graph-theoretical metrics via non-parametric ANOVA highlighted uncorrected group effects for bilateral betweenness centrality and right degree (Figure 5). *Post-hoc* tests indicated no statistically significant differences between TLE *never*-FBTCS and TLE *remote*-FBTCS for any metric at any network density level (all  $p>0.05$ , uncorrected across network densities within each metric). Plot inspection confirmed the previously documented pattern of higher centrality in TLE-FBTCS. Separate analyses for LTLE/RTLE subgroups are described in *Figure e-2* and *Appendix e-2*.

## DISCUSSION

In TLE, previous research documented thalamic involvement during temporal lobe seizures<sup>11, 36</sup> and identified thalamic atrophy<sup>5, 37</sup> along with altered structural and functional connectivity.<sup>38-40</sup> While much research focused on TLE as a whole, few investigations sought to identify markers of propensity for secondary generalization, and no studies investigated thalamic activation and connectivity during cognitive tasks. Using a verbal fluency fMRI paradigm, here we document coexistence of attenuated thalamic and hippocampal activation with stronger task-modulated thalamotemporal connectivity and higher thalamic centrality in TLE with active FBTCS, compared to TLE with focal seizures only. Current presence of FBTCS was defined based on the occurrence of such seizures in the year preceding the investigation, in accordance with established clinical recommendations.<sup>2, 3, 24</sup> *Post-hoc*

comparisons of patients with a history of remote FBTCS against those with no lifetime experience of secondary generalization detected no significant differences in thalamic profiles, suggesting that the identified thalamic functional abnormalities specifically relate to the presence of active, uncontrolled FBTCS. By challenging a functional network largely overlapping with the putative epileptogenic network of TLE, our findings indicate impaired thalamic functional profiles as potential candidate markers of recurrent FBTCS, and thus disease severity.

Analysis of task-related activation detected reduced anterior and posterior thalamic recruitment in TLE-FBTCS compared to TLE-FS, with greater significance on the left. Hippocampal activation was also lower in TLE-FBTCS. Corroborating our *a priori* hypotheses, these findings indicate task-related disengagement of key components of the pathologic network of TLE in the subgroup with FBTCS, emphasizing the involvement of the thalamus, and advancing preliminary evidence of suboptimal hippocampal recruitment during language in TLE.<sup>26</sup> From a neurobiological perspective, the fMRI signal relates to local field potentials, and likely reflects the extent of incoming input and local processes.<sup>41</sup> Hence, we hypothesize that repeated insults of secondarily generalized epileptic activity may lead to more marked derangements of local neural activity and affect richness of synaptic connections, which may in turn explain impaired task-related recruitment of both hippocampus and thalamus in TLE-FBTCS. Discrepancies of effects emerging from the comparisons between left and right TLE subgroups may relate to task specifics, as verbal fluency fMRI paradigms implicate linguistic processing, and are particularly suited to capture effects within left hemispheric networks.<sup>42</sup> Sensitivity analyses, including fluency scores as nuisance regressor, did not affect the results of the main group comparison and subgroup analyses, indicating that hippocampal and thalamic disengagement may occur during cognitive effort, but be independent of cognitive performance levels. We further confirmed subgroup comparability across a large series of clinical and demographic factors, including frontal and thalamic laterality indices. Moreover, multiple regression models identified FBTCS as the most significant determinant of anterior thalamic activation, among an extensive set of demographic, clinical and cognitive measures.

Analysis of fMRI activation identifies areas implicated in task execution, but does not formally capture the interplay between those areas, known as functional connectivity. To assess thalamotemporal connectivity during task-based fMRI, we conducted a psychophysiological interaction (PPI) analysis, providing measures of context-dependent,

task-modulated changes in coupling between a seed region and the whole-brain.<sup>31</sup> PPI analysis from both left and right thalamus demonstrated attenuation of task-related connectivity to fronto-temporo-parietal cortices and subcortical targets, in accordance with previous results in healthy controls.<sup>35</sup> Supporting a modulatory role of the thalamus during executive cognition, these findings relate to neurophysiological studies indicating thalamus-driven synchronization and mediation of cortico-cortical information transfer.<sup>43</sup> Group comparisons highlighted abnormal thalamotemporal interactions in TLE-FBTCS compared to FS, with less attenuated task-related connectivity between thalami and left hippocampus in the FBTCS subgroup, and altered connection between thalamus and anterior cingulate cortex. Stronger thalamotemporal coherence was particularly evident for comparisons of left TLE subgroups, whilst RTLE-FBTCS exhibited higher connectivity between thalamus and motor areas compared to RTLE-FS. Previous resting-state fMRI work in TLE documented bilaterally impaired connectivity of the posterior thalamus in TLE-FBTCS,<sup>12</sup> but correlated thalamic time-courses with those of cortical parcels with near-lobar extent. Here, we found that FBTCS relate to state-dependent connectivity differences affecting key components of the pathologic network of TLE, including limbic and rolandic areas. Task-based connectivity analysis thus provides an important complement to activation-based comparisons, by showing that reduced activation of hippocampus and thalamus is underpinned by stronger interregional synchrony and failure of reciprocal disengagement during cognition. From a mechanistic viewpoint, these findings may imply a reduced adaptability of neural communications within circuitry underlying secondary generalization, and highlight an association between recurrent FBTCS and more stereotyped, inflexible patterns of network interactions.

Graph-theoretical analysis allows tracking the organizational properties of brain networks, and centrality measures identify network *hubs*, i.e. regions with high connectivity to other network nodes and prominent influence over global network dynamics. In TLE, graph-theory investigations identified abnormalities of both mesiotemporal<sup>44</sup> and whole-brain network architecture.<sup>17</sup> Aberrant nodal topology was documented for limbic regions as well as thalamus,<sup>45</sup> and recent work reported higher thalamic centrality as predictor of post-surgical seizure recurrence.<sup>9</sup> Here, we identified higher anterior thalamic centrality in TLE-FBTCS compared to TLE-FS during a verbal fluency task, further supporting a relationship between FBTCS and higher thalamic functional integration within whole-brain networks. Our graph-theoretical results provide a third line of evidence for altered thalamic network embedding in

TLE-FBTCS relative to TLE-FS. Higher centrality likely implies stronger connectional profiles and enhanced thalamic relevance within the context of whole-brain network architecture,<sup>9</sup> which may underpin a network configuration facilitating diffuse dissemination of ictal discharges, and thus recurrent FBTCS.

To assess the potential clinical relevance of thalamic functional markers, we employed those within ROC curve analyses probing discrimination of TLE-FS and TLE-FBTCS. Though models already conveyed significant results with activation measures alone, discrimination abilities were substantially enhanced after combining measures of activity, connectivity and centrality into a composite thalamic functional construct, reaching 75% accuracy for all TLE, and >80% in LTLE. While proving the advantage of combining imaging metrics derived across investigative scales, these findings directly implicate thalamic functional profiles as potential surrogate marker of secondary generalization, with validity at the individual level.

Overall, our results dovetail with evidence from animal models, documenting the pivotal role of impaired thalamic gating for propagation and maintenance of seizures involving the neocortex,<sup>46</sup> and the efficacy of thalamotomy in suppressing the latter.<sup>47</sup> In patients with TLE, high-frequency thalamic stimulation desynchronizes hippocampal and large-scale epileptic network activity and induces cortico-cortical decoupling,<sup>48</sup> which may underlie the efficacy of deep brain anterior thalamic stimulation.<sup>49</sup> Our findings also complement recent resting-state fMRI evidence for abnormal interactions between thalamic divisions and basal ganglia in TLE with recent FBTCS.<sup>50</sup> While differing methodologically, both analyses compellingly indicate a prominent role of the thalamus in shaping susceptibility to uncontrolled secondary generalization in TLE.

In conclusion, our task-based fMRI investigation indicates reduced thalamic activation coupled with enhanced thalamotemporal connectivity and whole-brain thalamic network embedding as a functional signature of recurrent FBTCS in TLE. These patterns appear dynamic, and specifically relate to the presence of recent, uncontrolled secondary generalization. Altered thalamic network engagement is proposed as an imaging biomarker of active FBTCS, and thus disease severity, in TLE. While shedding light on the potential network correlates of recurrent FBTCS, our study delivers a viable target to track individual response to treatment, and assess efficacy of novel therapeutic strategies directed toward generalization of focal seizures and SUDEP.

**ACKNOWLEDGEMENTS**

We thank all our patients for their participation in this study, and the radiographers at the Epilepsy Society MRI Unit, Philippa Bartlett, Jane Burdett and Elaine Williams, for their help during data acquisition. We thank Mr. Jason Stretton for help with data acquisition, Drs. Britta Wandschneider and Urs Braun for helpful comments on an earlier version of the manuscript, Dr. Peter Zeidman (UCL Functional Imaging Group) for methodological input regarding psychophysiological interaction analysis, and Dr Aidan O’Keeffe for statistical advice. We also thank the anonymous reviewers for their suggestions to improve this manuscript.

**TABLE 1. Demographics, clinical characteristics and neuropsychological test results.**

	TLE (n= 113)			Left TLE (n= 55)			Right TLE (n= 58)		
	FS (n= 80)	FBTCS (n= 33)	P value	FS (n= 35)	FBTCS (n= 20)	P value	FS (n= 45)	FBTCS (n= 13)	P value
<i>Age</i> median (IQR), years	37.5 (18.0)	40.0 (18.5)	0.35	37.0 (18.0)	39.0 (19.5)	0.77	38.0 (17.5)	42.0 (13.0)	0.30
<i>Sex</i> (F/M, n)	54/26	19/14	0.32	21/14	9/11	0.39	33/12	10/3	1.00
<i>Handedness</i> L/R/ambidextrous (n)	10/66/4	4/29/0	0.42	4/30/1	2/18/0	1.00	6/36/3	2/11/0	1.00
<i>Age at onset</i> median (IQR), years	17.0 (15.0)	14.0 (13.5)	0.73	18.0 (16.0)	15.0 (13.5)	0.75	17.0 (15.5)	14.0 (16.5)	0.90
<i>Epilepsy duration</i> median (IQR), years	16.0 (20.3)	17.0 (26.0)	0.47	17.0 (17.0)	14.0 (30.3)	1.00	16.0 (24.5)	22.0 (18.5)	0.33
<i>Monthly focal seizure</i> <i>frequency</i> log. mean (SD)	0.9 (0.5)	0.9 (0.7)	0.99	0.94 (0.5)	0.90 (0.6)	0.80	0.86 (0.5)	0.89 (0.8)	0.88
<i>Lesional MRI</i> yes/no (n)	61/19	27/6	0.52	28/7	15/5	0.74	33/12	12/1	0.26
<i>Lesion type</i> none/HS/DNET/CAV, (n)	21/43/ 10/6	6/19/ 3/5	0.53	9/21/3/2	5/11/2/2	0.96	12/22/7/4	1/8/1/3	0.26
<i>AEDs</i> median (IQR)	2.0 (1.0)	2.0 (1.0)	0.58	2.0 (1.0)	2.0 (1.0)	0.81	2.0 (1.0)	3.0 (1.0)	0.23
<i>TPM/ZNS</i> yes/no (n)	16/64	6/27	1.00	10/25	4/16	0.54	6/39	2/11	1.00
<i>LEV</i> yes/no (n)	42/38	21/12	0.31	18/17	14/6	0.26	24/21	7/6	1.00
<i>Benzodiazepines</i> yes/no (n)	26/54	10/23	1.00	11/24	5/15	0.76	15/30	5/8	0.75
<i>Hippocampal volume</i> <i>ipsilateral, cc (SD)</i>	2.29 (0.6)	2.18 (0.6)	0.42	2.16 (0.6)	2.19 (0.7)	0.87	2.38 (0.6)	2.17 (0.4)	0.24
<i>Hippocampal volume</i> <i>contralateral, cc (SD)</i>	2.78 (0.3)	2.76 (0.4)	0.83	2.77 (0.3)	2.83 (0.4)	0.52	2.79 (0.2)	2.67 (0.3)	0.17
<i>Thalamic volume</i> <i>ipsilateral, cc (SD)</i>	6.15 (0.6)	6.08 (0.6)	0.52	6.17 (0.6)	5.94 (0.7)	0.19	6.13 (0.5)	6.30 (0.5)	0.32
<i>Thalamic volume</i> <i>contralateral, cc (SD)</i>	6.29 (0.5)	6.21 (0.5)	0.40	6.32 (0.5)	6.19 (0.6)	0.36	6.27 (0.4)	6.25 (0.3)	0.86
<i>NART IQ</i> mean (SD)	99.2 (11.9)	101.3 (15.0)	0.38	97.3 (12.2)	101.7 (14.6)	0.25	100.8 (11.7)	100.5 (16.5)	0.95
<i>Letter Fluency</i> mean (SD)	13.0 (5.6)	15.2 (5.2)	0.06	11.2 (4.6)	15.7 (4.6)	<b>0.01</b>	14.3 (6.0)	14.4 (6.2)	0.95
<i>Category Fluency</i> mean (SD)	18.1 (5.1)	18.9 (5.9)	0.55	17.7 (4.5)	19.8 (5.8)	0.14	18.5 (5.5)	17.3 (5.9)	0.50
<i>Graded Naming</i> mean (SD)	15.5 (5.6)	14.5 (6.3)	0.73	13.7 (5.7)	13.4 (6.5)	0.84	17.0 (5.1)	16.4 (5.6)	0.75
<i>Trail Making Test A</i> mean (SD)	35.3 (13.9)	32.3 (13.5)	0.18	34.2 (12.1)	31.3 (13.2)	0.24	36.1 (15.3)	34.3 (14.8)	0.57
<i>Trail Making Test B</i> mean (SD)	75.4 (32.6)	79.4 (32.7)	0.53	75.6 (30.5)	81.0 (36.8)	0.66	75.2 (34.6)	75.9 (23.3)	0.73
<i>BDI-FS score</i> median (IQR)	3.0 (4.0)	2.0 (5.0)	0.20	4.0 (4.0)	2.0 (4.0)	0.18	3.0 (3.3)	2.0 (6.5)	0.62
<i>BAI score</i> median (IQR)	10.0 (13.5)	8.50 (15.0)	0.72	10.0 (13.0)	4.0 (17.0)	0.15	10.0 (14.5)	15.0 (10.5)	0.41
<i>Lifetime history of</i> <i>affective disorder</i>	29/51	15/18	0.40	14/21	8/12	1.00	15/30	7/6	0.21

<i>yes/no (n)</i>									
<b><i>LI (frontal ROI)</i></b> <i>median (IQR)</i>	0.75 (0.4)	0.78 (0.4)	0.23	0.65 (0.3)	0.78 (0.4)	0.09	0.78 (0.5)	0.63 (0.5)	0.89
<b><i>LI (thalamus)</i></b> <i>median (IQR)</i>	0.52 (0.6)	0.49 (0.4)	0.96	0.55 (0.4)	0.48 (0.4)	0.62	0.45 (0.7)	0.56 (0.5)	0.71
<b><i>Framewise displacement (mm)</i></b> <i>mean (SD)</i>	0.09 (0.06)	0.10 (0.06)	0.27	0.09 (0.06)	0.09 (0.04)	0.79	0.09 (0.06)	0.11 (0.08)	0.18

**Abbreviations.** AED: anti-epileptic drug; BAI: Beck's Anxiety Inventory; BDI-FS: Beck Depression Inventory – Fast Screen; CAV: cavernoma; DNET: dysembryoplastic neuroepithelial tumor; FBTCS: patients with focal to bilateral tonic-clonic seizures; FS: patients with focal seizures only; HS: hippocampal sclerosis; IQR: interquartile range; LI: laterality index; NART: National Adult Reading Test; ROI: region of interest; SD: standard deviation; TLE: temporal lobe epilepsy; TPM: topiramate; ZNS: zonisamide. Neuropsychological measures are reported as raw scores. Letter and category fluency data were missing for four patients. Statistics for Trail Making Test A and B were carried out on log-transformed data, but raw data are provided in the table to ensure comparability with published literature. *P* values not in bold (i.e., all but one, as detailed below) are uncorrected for multiple comparisons. The only *p* value in bold (letter fluency, LTLE-FBTCS versus LTLE-FS) is FDR-adjusted across six cognitive measures (IQ, letter fluency, category fluency, naming, Trail Making Test A and B; uncorrected *p* value= 0.002). Framewise displacement values were computed according to the formula by Jenkinson and collaborators, implemented in DPARSF for SPM12.<sup>e13</sup>

**TABLE 2. Comparisons of TLE-FBTCS and TLE-FS for verbal fluency activation and PPI analyses: anatomical locations and statistical descriptors.**

	<i>Left Hemisphere</i>			<i>Right Hemisphere</i>		
	MNI coordinates (x,y,z)	Z-score	P value	MNI coordinates (x,y,z)	Z-score	P value
<b><i>TLE - FS &gt; FBTCS</i></b>						
<b><i>Verbal fluency activations</i></b>						
<i>Anterior thalamus (ventral anterior)</i>	-9 -4 -1	3.35 [3.13]	<b>0.005*</b> <b>[0.01*]</b>	15 -7 8	3.09 [2.65]	<b>0.011*</b> <b>[0.034*]</b>
<i>Posterior thalamus (centrolateral/ lateral posterior)</i>	-12 -22 14	2.94 [2.71]	<b>0.016*</b> <b>[0.029*]</b>	6 -22 8	2.88 [2.30]	<b>0.019*</b> <b>[0.071]</b>
<i>Posterior thalamus (medial geniculate)</i>	-15 -28 -7	2.84 [2.35]	<b>0.021*</b> <b>[0.065]</b>			
<i>Hippocampus</i>	-30 -16 -16	2.82 [2.30]	<b>0.022*</b> <b>[0.078]</b>			
<i>Putamen</i>				24 8 -13	3.29 [3.04]	0.001 [0.001]
<i>Pallidum</i>	-15 -10 -7	3.36 [2.72]	<0.001 [0.003]			
<i>Ventral diencephalon (subthalamus)</i>	-12 -19 -10	3.14	0.001	6 -28 -10	3.51 [2.59]	<0.001 [0.005]
<i>Posterior parahippocampal gyrus</i>	-15 -37 -4	3.28 [2.80]	0.001 [0.003]	18 -34 -7	3.70 [2.96]	<0.001 [0.002]
<i>Cerebellum</i>				6 55 -10	3.18 [3.04]	0.001 [0.001]
<b><i>Left thalamic PPI</i></b>						
<b><i>TLE - FBTCS &gt; FS</i></b>						
<i>Left hippocampus</i>	-36 -19 -16	2.77 [3.13]	<b>0.028*</b> <b>[0.011*]</b>			
<i>Precentral gyrus</i>	-21 -16 53	2.53 [3.31]	<b>0.049*</b> <b>[0.006*]</b>	27 -19 65	2.78 [3.13]	<b>0.027*</b> <b>[0.011*]</b>
<i>Supplementary motor area</i>				3 11 50	2.70 [3.31]	<b>0.033*</b> <b>[0.006*]</b>
<i>Superior frontal gyrus</i>				18 20 41	3.22 [3.61]	0.001 [<0.001]
<i>Anterior cingulate cortex</i>				3 32 8	2.92 [3.01]	0.002 [0.001]
<i>Insula/posterior parietal operculum</i>	-36 -25 29	3.37 [3.72]	<0.001 [<0.001]			
<b><i>Right thalamic PPI</i></b>						
<b><i>TLE - FBTCS &gt; FS</i></b>						
<i>Hippocampus</i>	-27 -25 16	2.91 [3.09]	<b>0.018*</b> <b>[0.011*]</b>			
<i>Amygdala</i>	-27 -1 -22	2.91 [3.11]	<b>0.019*</b> <b>[0.010*]</b>			

Coordinates of group-wise activation and PPI differences are given in MNI space. Coordinates of group-wise peak left thalamic activation for seed-based left PPI analysis:  $x=-9$ ,  $y=-4$ ,  $z=-8$ ,  $z\text{-score}=\infty$ ; coordinates of group-wise peak right thalamic activation for seed-based right PPI analysis:  $x=9$ ,  $y=-1$ ,  $z=5$ ,  $z\text{-score}=7.49$ .  $Z$  scores and  $p$  values within square brackets are those obtained via sensitivity analyses using letter fluency scores as nuisance regressors. When in bold,  $p$  values for peak-level differences in thalamic and hippocampal activation, interthalamic, thalamotemporal and thalamo-motor connectivity are FWE-corrected for multiple comparisons, using a 12-mm diameter spherical ROI centred on the local maximum; asterisks denote statistical significance ( $p<0.05$ , FWE-svc).  $P$  values not in bold are uncorrected for multiple comparisons across the whole brain.

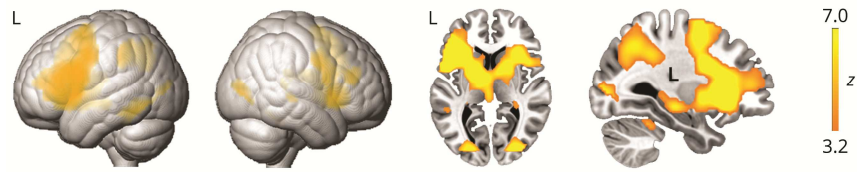
ACCEPTED

## FIGURE LEGENDS

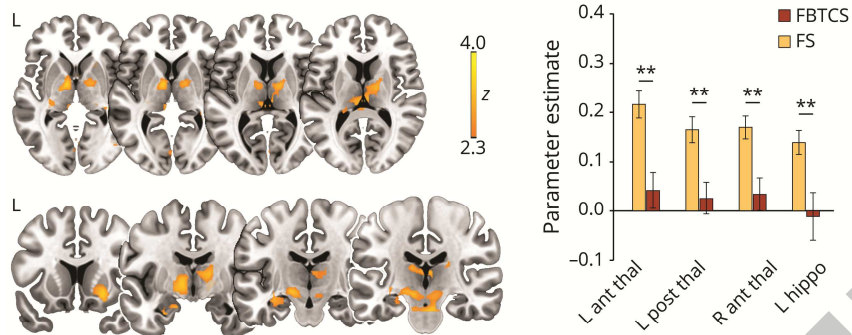
### Figure 1. Verbal fluency fMRI activations.

Panel A shows whole-brain verbal fluency activations across all participants, as derived from one-sample *t*-tests. Axial and sagittal slices highlight activation of the thalamus, basal ganglia and hippocampus. Panels B to D display comparisons between TLE-FS and TLE-FBTCS for task-related activation (B), and repeat contrasts for the same subgroups in left (C) and right (D) TLE. Axial slices specifically highlight differences in thalamic activation. Across panels B to D, bar graphs display SPM-derived parameter estimates of thalamic activation for areas of peak intergroup differences, namely: left anterior/posterior thalamus, right anterior thalamus and left hippocampus for TLE-FBTCS versus TLE-FS (B); all the former plus right hippocampus for LTLE subgroups (C); left/right anterior thalamus for RTLE subgroups (D); in the latter case, thalamic activation differences did not reach statistical significance, but bar graphs are reported for completeness. Rendered images in Panel A are thresholded at  $p < 0.05$ , FWE-corrected for multiple comparisons across the whole brain. Across all panels, heat maps refer to brain slices, and display *z*-scores. MNI coordinates and *p* values for group comparisons are provided in Table 2 and Table e-1. In bar graphs: \*\*,  $p < 0.05$ , FWE-svc for peak intergroup difference.

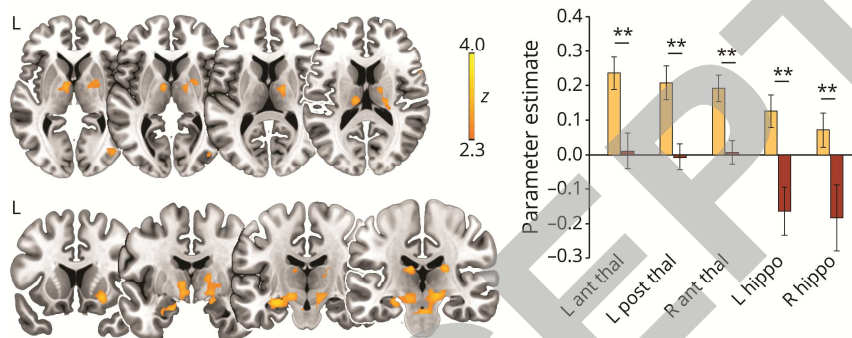
A. Task effects



B. TLE - FBTCs < FS



C. LTLE - FBTCs < FS



D. RTLE - FBTCs < FS

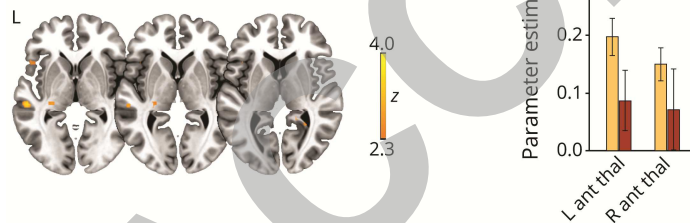


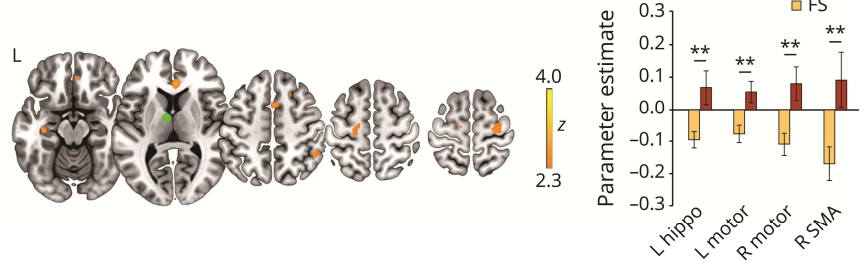
**Figure 2. Psychophysiological interaction analysis - left thalamus.**

Panel A shows task-modulated changes in left anterior thalamic connectivity across all participants. The green sphere in the axial slice corresponds to the left thalamic seed. Panels B to D display comparisons between TLE-FBTCS and TLE-FS (B), and repeat contrasts for the same subgroups in left (C) and right (D) TLE. Across panels B to D, bar graphs on the right display SPM-derived parameter estimates of left thalamic PPI for areas of peak intergroup differences, namely: left hippocampus, left/right precentral gyrus (motor cortex) and right SMA for TLE-FBTCS versus TLE-FS (B); left hippocampus (two spatially non-contiguous peaks), left SMA and right medial dorsal thalamus for LTLE subgroups (C); left/right precentral gyrus (motor cortex; two spatially non-contiguous peaks on both sides) for RTLE subgroups (D). Rendered images in Panel A are thresholded at  $p < 0.001$ , uncorrected for illustration purposes. Across all panels, heat maps refer to brain slices, and display z-scores. MNI coordinates and  $p$  values for group comparisons are provided in Table 2 and Table e-1. In bar graphs: \*\*,  $p < 0.05$ , FWE-svc for peak between-group difference.

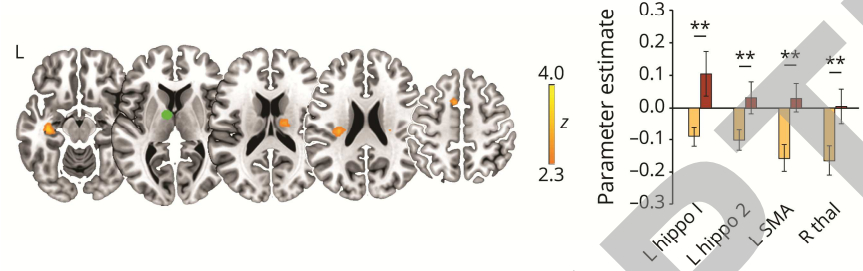
A. Task-modulated connectivity



B. TLE - FBTCS > FS



C. LTLE - FBTCS > FS



D. RTLE - FBTCS > FS

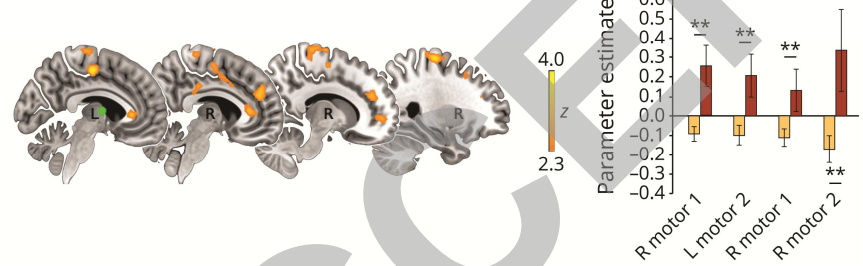


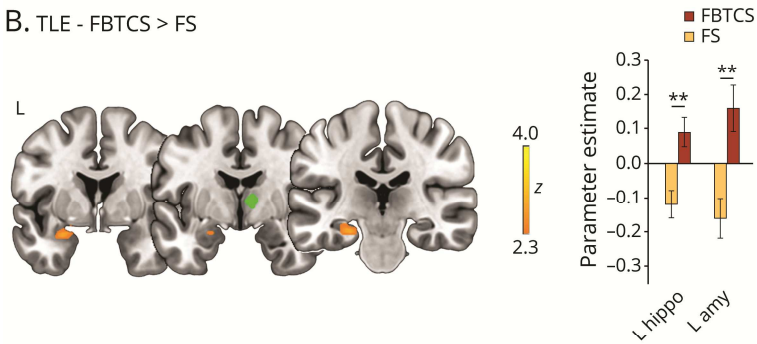
**Figure 3. Psychophysiological interaction analysis - right thalamus.**

Panel A shows task-modulated changes in right anterior thalamic connectivity across all participants. The green sphere in the axial slice shows the upper portion of the right thalamic seed. Panels B to D display comparisons between TLE-FBTCS and TLE-FS (B), and repeat contrasts for the same subgroups in left (C) and right TLE (D). For panels B to D, bar graphs on the right display SPM-derived parameter estimates of right thalamic PPI for areas of peak intergroup differences, corresponding to left hippocampus and left amygdala for all group comparisons. As for analyses in RTLE, bar graphs are reported for completeness, but group differences for hippocampal and amygdala's activity did not reach statistical significance. Rendered images in Panel A are thresholded at  $p < 0.001$ , uncorrected for illustration purposes. Across all panels, heat maps refer to brain slices, and display z-scores. MNI coordinates and  $p$  values for group comparisons are provided in Table 2 and Table e-1. In bar graphs: \*\*,  $p < 0.05$ , FWE-svc for peak between-group difference.

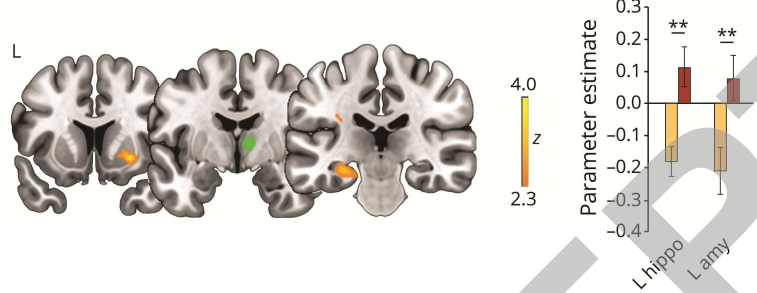
## A. Task-modulated connectivity



## B. TLE - FBTCs &gt; FS



## C. LTLE - FBTCs &gt; FS



## D. RTLE - FBTCs &gt; FS

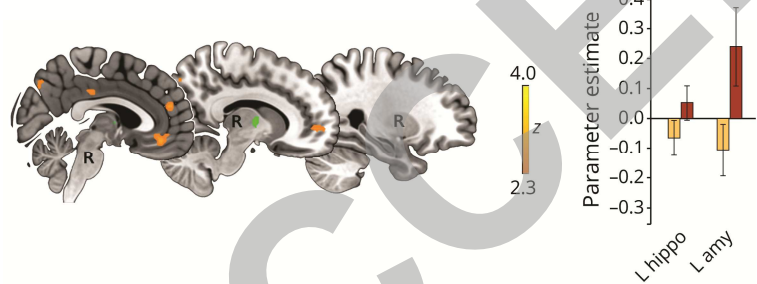


#### Figure 4. Graph-theoretical measures of centrality.

Panels A-C display measures of betweenness and degree centrality of the left and right thalamic ROI. Metrics for FBTCS and FS patient groups are displayed with dark red and orange lines, respectively. Shaded bands display standard errors, red dots indicate significant intergroup differences after FDR correction for multiple comparisons ( $p_{\text{FDR}} < 0.05$ ), grey dots indicate between-group differences at  $p < 0.05$ , uncorrected for multiple comparisons.

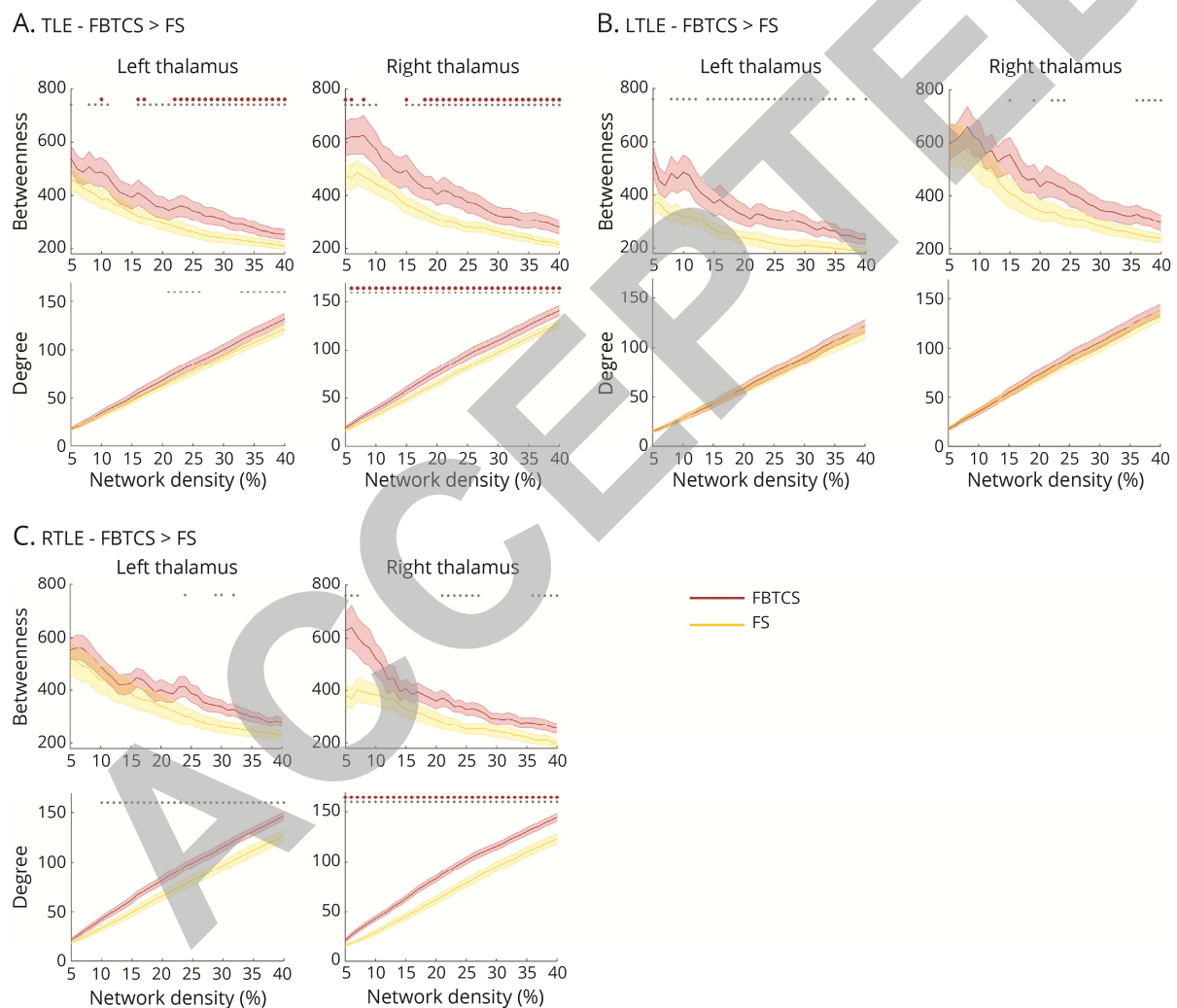
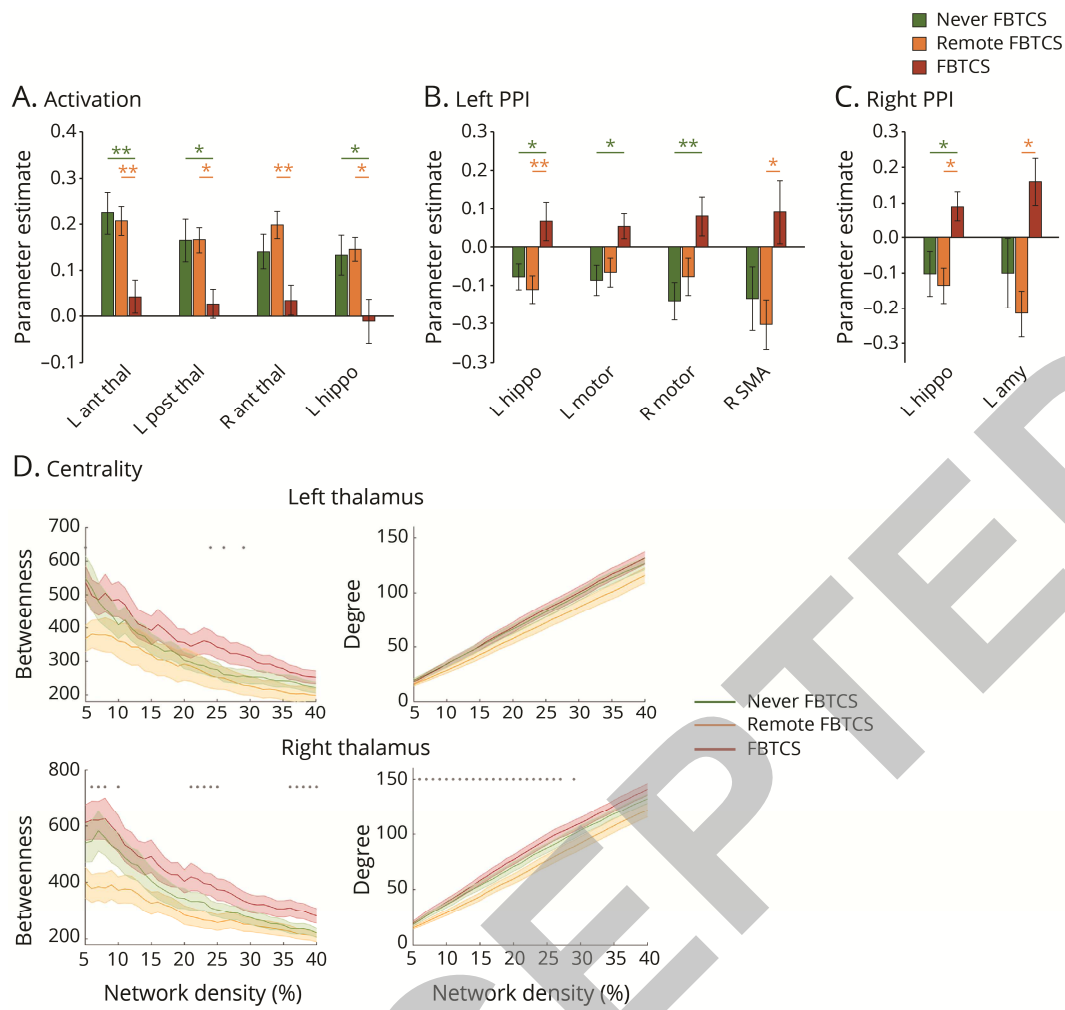


**Figure 5. Post-hoc analyses on three TLE groups.**

Panels A-D illustrate comparisons among (1) TLE with (current) FBTCS, corresponding to the group termed TLE-FBTCS throughout the manuscript, (2) TLE *remote*-FBTCS and (3) TLE *never*-FBTCS (for further grouping details, see *Methods*). Bar graphs in panels A to C display parameter estimates extracted from locations of peak group differences in the main analysis on two groups, corresponding to: left anterior/posterior thalamus, right anterior thalamus and left hippocampus for thalamic activation, panel A; left hippocampus, left/right precentral gyrus (motor cortex) and right SMA for left thalamic PPI, panel B; left hippocampus and amygdala for right thalamic PPI, panel C. MNI coordinates of each location are provided in Tables 2 and e-1. Panel D shows group comparisons for measures of betweenness and degree centrality of the left and right thalamic ROI. Shaded bands display standard errors, grey dots indicate between-group differences at  $p < 0.05$ , uncorrected for multiple comparisons. There were no significant intergroup differences after correction for multiple testing. In bar graphs: \*\*,  $p < 0.01$ ; corrected (Tukey); \*,  $p < 0.05$ , corrected (Tukey).



**APPENDIX 1: AUTHORS**

<b>NAME</b>	<b>LOCATION</b>	<b>CONTRIBUTION</b>
Lorenzo Caciagli, MD, PhD	Queen Square, London, and Chalfont St Peter, UK	Study concept and design, analysis and interpretation of data including statistical analysis, drafting and revision of manuscript for intellectual content
Luke Allen, PhD	Queen Square, London, and Chalfont St Peter, UK	Analysis of data, revision of manuscript for intellectual content
Xiaosong He, PhD	University of Pennsylvania, Philadelphia, USA	Interpretation of data, revision of manuscript for intellectual content
Karin Trimmel, MD, PhD	Queen Square, London, and Chalfont St Peter, UK, and Vienna, Austria	Interpretation of data, revision of manuscript for intellectual content
Sjoerd B. Vos, PhD	Queen Square, London, and Chalfont St Peter, UK	Contribution of data analysis scripts, revision of manuscript for intellectual content
Maria Centeno, MD, PhD	Queen Square, London, and Chalfont St Peter, UK	Acquisition of data, revision of manuscript for intellectual content
Marian Galovic, MD	Queen Square, London, and Chalfont St Peter, UK	Revision of manuscript for intellectual content
Meneka K. Sidhu, MBChB, PhD, MRCP	Queen Square, London, and Chalfont St Peter, UK	Acquisition of data, revision of manuscript for intellectual content
Pamela J. Thompson, PhD	Queen Square, London, and Chalfont St Peter, UK	Acquisition of data, revision of manuscript for intellectual content
Danielle S. Bassett, PhD	University of Pennsylvania, Philadelphia, USA	Consulting on statistics, interpretation of data, revision of manuscript for intellectual content
Gavin P. Winston, BM BCh, PhD, MRCP	Queen Square, London, and Chalfont St Peter, UK, and Kingston, Ontario, Canada	Acquisition of data, revision of manuscript for intellectual content
John S. Duncan, DM, FRCP	Queen Square, London, and Chalfont St Peter, UK	Study supervision, interpretation of data, revision of manuscript for intellectual content, obtainment of funding
Matthias J. Koepp, MD, PhD, FRCP	Queen Square, London, and Chalfont St Peter, UK	Study concept or design, study supervision, interpretation of data, revision of manuscript for intellectual content, obtainment of funding
Michael R. Sperling, MD	Thomas Jefferson University, Philadelphia, USA	Study concept or design, study supervision, analysis and interpretation of data, revision of manuscript for intellectual content

**REFERENCES**

1. Jobst BC, Williamson PD, Neuschwander TB, Darcey TM, Thadani VM, Roberts DW. Secondly generalized seizures in mesial temporal epilepsy: clinical characteristics, lateralizing signs, and association with sleep-wake cycle. *Epilepsia* 2001;42:1279-1287.
2. Walczak TS, Leppik IE, D'Amelio M, et al. Incidence and risk factors in sudden unexpected death in epilepsy: a prospective cohort study. *Neurology* 2001;56:519-525.
3. Nilsson L, Farahmand BY, Persson PG, Thiblin I, Tomson T. Risk factors for sudden unexpected death in epilepsy: a case-control study. *Lancet* 1999;353:888-893.
4. Janszky J, Janszky I, Schulz R, et al. Temporal lobe epilepsy with hippocampal sclerosis: predictors for long-term surgical outcome. *Brain* 2005;128:395-404.
5. Barron DS, Fox PM, Laird AR, Robinson JL, Fox PT. Thalamic medial dorsal nucleus atrophy in medial temporal lobe epilepsy: A VBM meta-analysis. *NeuroImage Clinical* 2012;2:25-32.
6. Bernhardt BC, Bernasconi N, Kim H, Bernasconi A. Mapping thalamocortical network pathology in temporal lobe epilepsy. *Neurology* 2012;78:129-136.
7. Mueller SG, Laxer KD, Barakos J, et al. Involvement of the thalamocortical network in TLE with and without mesiotemporal sclerosis. *Epilepsia* 2010;51:1436-1445.
8. Keller SS, Richardson MP, Schoene-Bake JC, et al. Thalamotemporal alteration and postoperative seizures in temporal lobe epilepsy. *Annals of neurology* 2015;77:760-774.
9. He X, Doucet GE, Pustina D, Sperling MR, Sharan AD, Tracy JI. Presurgical thalamic "hubness" predicts surgical outcome in temporal lobe epilepsy. *Neurology* 2017;88:2285-2293.
10. Norden AD, Blumenfeld H. The role of subcortical structures in human epilepsy. *Epilepsy & behavior : E&B* 2002;3:219-231.
11. Bertram EH, Mangan PS, Zhang D, Scott CA, Williamson JM. The midline thalamus: alterations and a potential role in limbic epilepsy. *Epilepsia* 2001;42:967-978.
12. He X, Doucet GE, Sperling M, Sharan A, Tracy JI. Reduced thalamocortical functional connectivity in temporal lobe epilepsy. *Epilepsia* 2015;56:1571-1579.
13. Chen C, Li H, Ding F, et al. Alterations in the hippocampal-thalamic pathway underlying secondarily generalized tonic-clonic seizures in mesial temporal lobe epilepsy: A diffusion tensor imaging study. *Epilepsia* 2019;60:121-130.
14. Saalman YB, Kastner S. The cognitive thalamus. *Frontiers in systems neuroscience* 2015;9:39.
15. Schmitt LI, Wimmer RD, Nakajima M, Happ M, Mofakham S, Halassa MM. Thalamic amplification of cortical connectivity sustains attentional control. *Nature* 2017;545:219-223.
16. Cole MW, Bassett DS, Power JD, Braver TS, Petersen SE. Intrinsic and task-evoked network architectures of the human brain. *Neuron* 2014;83:238-251.
17. Caciagli L, Bernhardt BC, Hong SJ, Bernasconi A, Bernasconi N. Functional network alterations and their structural substrate in drug-resistant epilepsy. *Front Neurosci* 2014;8:411.
18. He X, Bassett DS, Chaitanya G, Sperling MR, Kozlowski L, Tracy JI. Disrupted dynamic network reconfiguration of the language system in temporal lobe epilepsy. *Brain* 2018;141:1375-1389.
19. Szaflarski JP, Gloss D, Binder JR, et al. Practice guideline summary: Use of fMRI in the presurgical evaluation of patients with epilepsy: Report of the Guideline Development, Dissemination, and Implementation Subcommittee of the American Academy of Neurology. *Neurology* 2017;88:395-402.

20. Wagner S, Sebastian A, Lieb K, Tuscher O, Tadic A. A coordinate-based ALE functional MRI meta-analysis of brain activation during verbal fluency tasks in healthy control subjects. *BMC Neurosci* 2014;15:19.
21. Yarkoni T, Poldrack RA, Nichols TE, Van Essen DC, Wager TD. Large-scale automated synthesis of human functional neuroimaging data. *Nat Methods* 2011;8:665-670.
22. Winston GP, Cardoso MJ, Williams EJ, et al. Automated hippocampal segmentation in patients with epilepsy: available free online. *Epilepsia* 2013;54:2166-2173.
23. Stretton J, Pope RA, Winston GP, et al. Temporal lobe epilepsy and affective disorders: the role of the subgenual anterior cingulate cortex. *J Neurol Neurosurg Psychiatry* 2015;86:144-151.
24. Engel J, Jr., Wiebe S, French J, et al. Practice parameter: temporal lobe and localized neocortical resections for epilepsy: report of the Quality Standards Subcommittee of the American Academy of Neurology, in association with the American Epilepsy Society and the American Association of Neurological Surgeons. *Neurology* 2003;60:538-547.
25. Xiao F, Caciagli L, Wandschneider B, et al. Effects of carbamazepine and lamotrigine on functional magnetic resonance imaging cognitive networks. *Epilepsia* 2018;59:1362-1371.
26. Bonelli SB, Powell R, Thompson PJ, et al. Hippocampal activation correlates with visual confrontation naming: fMRI findings in controls and patients with temporal lobe epilepsy. *Epilepsy research* 2011;95:246-254.
27. Sidhu MK, Stretton J, Winston GP, et al. A functional magnetic resonance imaging study mapping the episodic memory encoding network in temporal lobe epilepsy. *Brain : a journal of neurology* 2013;136:1868-1888.
28. Wandschneider B, Burdett J, Townsend L, et al. Effect of topiramate and zonisamide on fMRI cognitive networks. *Neurology* 2017;88:1165-1171.
29. Lieberman MD, Cunningham WA. Type I and Type II error concerns in fMRI research: re-balancing the scale. *Social cognitive and affective neuroscience* 2009;4:423-428.
30. Krauth A, Blanc R, Poveda A, Jeanmonod D, Morel A, Szekely G. A mean three-dimensional atlas of the human thalamus: generation from multiple histological data. *Neuroimage* 2010;49:2053-2062.
31. Friston KJ, Buechel C, Fink GR, Morris J, Rolls E, Dolan RJ. Psychophysiological and modulatory interactions in neuroimaging. *NeuroImage* 1997;6:218-229.
32. Zeidman P, Jafarian A, Corbin N, et al. A guide to group effective connectivity analysis, part 1: First level analysis with DCM for fMRI. *Neuroimage* 2019;200:174-190.
33. Fan L, Li H, Zhuo J, et al. The Human Brainnetome Atlas: A New Brain Atlas Based on Connectional Architecture. *Cereb Cortex* 2016;26:3508-3526.
34. Bassett DS, Bullmore E, Verchinski BA, Mattay VS, Weinberger DR, Meyer-Lindenberg A. Hierarchical organization of human cortical networks in health and schizophrenia. *J Neurosci* 2008;28:9239-9248.
35. O'Muircheartaigh J, Vollmar C, Barker GJ, et al. Abnormal thalamocortical structural and functional connectivity in juvenile myoclonic epilepsy. *Brain : a journal of neurology* 2012;135:3635-3644.
36. Guye M, Regis J, Tamura M, et al. The role of corticothalamic coupling in human temporal lobe epilepsy. *Brain : a journal of neurology* 2006;129:1917-1928.
37. Keller SS, Roberts N. Voxel-based morphometry of temporal lobe epilepsy: An introduction and review of the literature. *Epilepsia* 2008;49:741-757.
38. Keller SS, O'Muircheartaigh J, Traynor C, Towgood K, Barker GJ, Richardson MP. Thalamotemporal impairment in temporal lobe epilepsy: a combined MRI analysis of structure, integrity, and connectivity. *Epilepsia* 2014;55:306-315.

39. Dinkelacker V, Valabregue R, Thivard L, et al. Hippocampal-thalamic wiring in medial temporal lobe epilepsy: Enhanced connectivity per hippocampal voxel. *Epilepsia* 2015;56:1217-1226.
40. Barron DS, Fox PT, Pardoe H, et al. Thalamic functional connectivity predicts seizure laterality in individual TLE patients: application of a biomarker development strategy. *NeuroImage Clinical* 2015;7:273-280.
41. Logothetis NK, Pauls J, Augath M, Trinath T, Oeltermann A. Neurophysiological investigation of the basis of the fMRI signal. *Nature* 2001;412:150-157.
42. Bonelli SB, Thompson PJ, Yogarajah M, et al. Imaging language networks before and after anterior temporal lobe resection: results of a longitudinal fMRI study. *Epilepsia* 2012;53:639-650.
43. Sherman SM. Thalamus plays a central role in ongoing cortical functioning. *Nat Neurosci* 2016;19:533-541.
44. Bernhardt BC, Bernasconi N, Hong SJ, Dery S, Bernasconi A. Subregional Mesiotemporal Network Topology Is Altered in Temporal Lobe Epilepsy. *Cereb Cortex* 2016;26:3237-3248.
45. Vaughan DN, Rayner G, Tailby C, Jackson GD. MRI-negative temporal lobe epilepsy: A network disorder of neocortical connectivity. *Neurology* 2016;87:1934-1942.
46. Paz JT, Davidson TJ, Frechette ES, et al. Closed-loop optogenetic control of thalamus as a tool for interrupting seizures after cortical injury. *Nat Neurosci* 2013;16:64-70.
47. Mondragon S, Lamarche M. Suppression of motor seizures after specific thalamotomy in chronic epileptic monkeys. *Epilepsy Res* 1990;5:137-145.
48. Yu T, Wang X, Li Y, et al. High-frequency stimulation of anterior nucleus of thalamus desynchronizes epileptic network in humans. *Brain* 2018;141:2631-2643.
49. Salanova V, Witt T, Worth R, et al. Long-term efficacy and safety of thalamic stimulation for drug-resistant partial epilepsy. *Neurology* 2015;84:1017-1025.
50. He X, Chaitanya G, Asma B, et al. Disrupted basal ganglia-thalamocortical loops in focal to bilateral tonic-clonic seizures. *Brain* 2020;143:175-190.

# Neurology®

## Thalamus and focal to bilateral seizures: A multi-scale cognitive imaging study

Lorenzo Caciagli, Luke A. Allen, Xiaosong He, et al.

*Neurology* published online August 26, 2020

DOI 10.1212/WNL.0000000000010645

**This information is current as of August 26, 2020**

<b>Updated Information &amp; Services</b>	including high resolution figures, can be found at: <a href="http://n.neurology.org/content/early/2020/08/26/WNL.0000000000010645.full">http://n.neurology.org/content/early/2020/08/26/WNL.0000000000010645.full</a>
<b>Subspecialty Collections</b>	This article, along with others on similar topics, appears in the following collection(s): <b>fMRI</b> <a href="http://n.neurology.org/cgi/collection/fmri">http://n.neurology.org/cgi/collection/fmri</a>
<b>Permissions &amp; Licensing</b>	Information about reproducing this article in parts (figures, tables) or in its entirety can be found online at: <a href="http://www.neurology.org/about/about_the_journal#permissions">http://www.neurology.org/about/about_the_journal#permissions</a>
<b>Reprints</b>	Information about ordering reprints can be found online: <a href="http://n.neurology.org/subscribers/advertise">http://n.neurology.org/subscribers/advertise</a>

*Neurology*® is the official journal of the American Academy of Neurology. Published continuously since 1951, it is now a weekly with 48 issues per year. Copyright © 2020 The Author(s). Published by Wolters Kluwer Health, Inc. on behalf of the American Academy of Neurology. All rights reserved. Print ISSN: 0028-3878. Online ISSN: 1526-632X.

